Field-Induced Electron-Ion Recombination: A Novel Route towards Neutral (Anti-)matter

C. Wesdorp,[1] F. Robicheaux,[2] and L. D. Noordam[1]

[1]*FOM Institute for Atomic and Molecular Physics, Kruislaan 407, 1098 SJ, Amsterdam, The Netherlands*

[2]*Department of Physics, Auburn University, Auburn, Alabama 36849*

(Received 10 November 1999)

We present a novel approach to the preparation of neutral (anti-)matter. The scheme is based on recombination of a free electron and an ion, and can be considered as the inverse of pulsed field ionization. We have obtained promising results on rubidium: at low densities already efficiencies of 0.3% were obtained. This is orders of magnitude more than has been achieved in previous recombination studies.

PACS numbers: 32.80.Rm, 78.60.–b, 79.70.+q

The recombination of an antiproton with a positron is one of the hurdles in the process of making neutral antihydrogen atoms. Existing recombination schemes for the formation of neutral atoms such as dielectronic recombination [1] and dissociative recombination [2] cannot be used due to the absence of internal structure of the (anti-)proton. Recombination of a proton and an electron to form an atom is possible only when a third body takes away the excess energy of the captured electron. This third body can be a spectator, in which case this mechanism is known as three body recombination (TBR) [1]. In order to achieve sizeable recombination rates TBR is studied in high density plasmas at low temperatures (~4 K) [3]. When this third body is a photon, this mechanism is known as radiative recombination (RR) [4]. RR can be stimulated by a laser field (stimulated radiative recombination, SRR [5]) and becomes more efficient for lower laser frequencies (scaling as ν^{-3}) and temperature of the plasmas.

Here we present a third and efficient mechanism for the recombination of free electrons with free ions, using pulsed electric fields ($\nu \sim 0.1$ GHz). The scheme is schematically sketched in the upper panel of Fig. 1. An ion is situated in a static electric field. The static electric field modifies the Coulomb potential such that a saddle point is created (Fig. 1a). If an electron passes over the saddle point in the modified Coulomb potential, it will take a small, but not negligible, amount of time to return to the saddle point and escape from the ion (Fig. 1a). If the static field is turned off (Fig. 1b) before the electron returns to the saddle point, it will remain bound in a highly excited state (Fig. 1c). In the experiments reported in this Letter the electrons start out with a kinetic energy of 0.75 eV and are decelerated by a static electric field of 1.5 V/cm, such that the electrons have their turning at the position of a rubidium ion source. The time required for the electron to travel from the saddle point, to the rubidium nucleus, and back to the saddle point is roughly 1 ns for the fields and energies used in this experiment. In Fig. 1d the experimentally determined efficiency (number of recombined rubidium atoms divided by the number of free rubidium ions) of this scheme is depicted as a function of the delay of the fast field turnoff. This delay is with respect to the time when the free electron has its turning point in the electric field. Clearly, a maximum number of recombination events is recorded at zero delay. Note that efficiencies up to 2.9×10^{-3} are obtained.

We will argue why this scheme of pulsed field recombination (PFR) can work for any atom. PFR does not rely on core scattering, arising from quantum defects of nonhydrogenic atoms [6]. As we show later, the PFR scheme produces an atom in a Rydberg state [6], a state with a high principal quantum number ($n \approx 200$). PFR can be viewed as the inverse process of pulsed-field ionization [6], in which a pulsed electric field ionizes a Rydberg state.

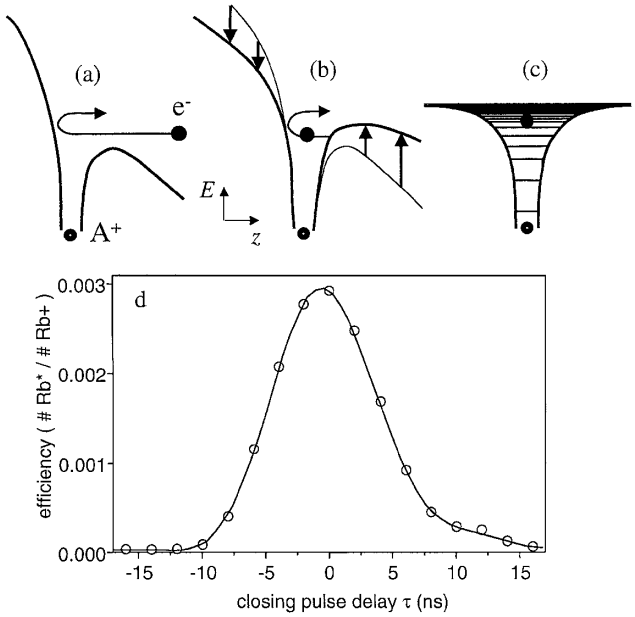

FIG. 1. Schematic representation of the pulsed field recombination scheme: (a) An ion awaits in a static electric field an electron, which is decelerated and has its turning point at the ion. (b) When the electron is at the turning point, the electric field is quickly turned off. (c) If the field is turned off during the turning of the electron, a bound state is formed. (d) Experimentally observed efficiency (number of recombined atoms divided by the number of free Rb ions) as a function of the delay (τ) of the quick turnoff (1.5 to 0.2 V/cm in 1.0 ns).

The latter process is used in atomic physics to determine the principal quantum number of a Rydberg state [7], and in physical chemistry it forms the basis of ZEKE spectroscopy [8], determining the photoionization potential of large molecules.

The PFR scheme was experimentally realized as follows: a pulsed electron source [9] was created by photoionizing lithium atoms in a static electric field of 1.50 V/cm, with a pulsed (9 ns duration) narrow band ($\Delta\lambda < 0.2$ cm^{-1}) dye laser (operating at 30 Hz). Typically electron pulses of 9 ns duration, with about $(5 \pm 2) \times 10^4$ electrons in a volume of 0.02 mm^3 were produced. The electric field is created by two parallel capacitor plates (separation: 10.0 mm) over which a voltage is applied (Fig. 2). The ionizing laser pulse is focused to a diameter of 50 μm to minimize the energy spread of the created electron pulses. After ionization, the free electrons are pushed towards the anode plate (connected to ground) through which a small hole is drilled, covered by a grid. After passing through the anode, the electrons enter a field-free region of 15.0 mm, after which another set of parallel capacitor plates (with small holes, covered by a grid) is situated. Since the final plate is on -1.50 V the electrons turn around halfway between these plates, separated by 10.0 mm. In this region a cloud of rubidium ions is awaiting the electrons. To minimize the spread of the electrons during their travel towards the ions in directions perpendicular to the direction of propagation, a magnetic field was implemented, parallel to the direction of propagation ($B_z = 2.5$ mT). Typically $(5 \pm 2) \times 10^3$ Rb ions were produced in a volume of 2.0 mm^3. The ions were produced by photoionizing rubidium atoms in a static electric field of 1.50 V/cm, 50 ns before the lithium atoms were ionized, in a two-photon process. The frequency doubled output of a Nd:YAG laser was used for this two-photon process (2×532 nm), resulting in ionized electrons with an initial velocity of 4×10^5 m/s. Therefore, all the electrons originating from ionized rubidium atoms have left this interaction region at the time the lithium photoelectrons are created. Note that the heavy rubidium ions are virtually standing still during our experiment ($\Delta l = 1$ μm in 100 ns). The shape of the ion cloud is ~6 mm in the z and x direction, and 60 μm in the y direction. In the ion source region the electrons are decelerated by the electric field of 1.50 V/cm, and have their turning point at the position of the ion cloud. At that time the field is turned off by dipping the voltage on the cathode plate from -1.50 to -0.20 V. The electric field turnoff is realized by connecting an impedance matched, fast pulse generator to the cathode plate. Different pulse generators were used to study the effect of different fall times of the electric field (90% → 10% in 0.4 ns, 1.0 ns, and 9.0 ns, respectively). The number of Rb ions is kept low with respect to the number of free electrons to prevent the effect of "trapping" the electrons in the attractive potential of the ions. For 5×10^3 ions in a sphere with a volume of 2.0 mm^3, the electrons feel an attractive field of 110 mV/cm at the edge of this sphere. Such a low density plasma is therefore not stable when the ion region is biased after the quick turnoff to an electric field of 200 mV/cm. The experiments were performed in a vacuum chamber with a background pressure of 5×10^{-7} Torr.

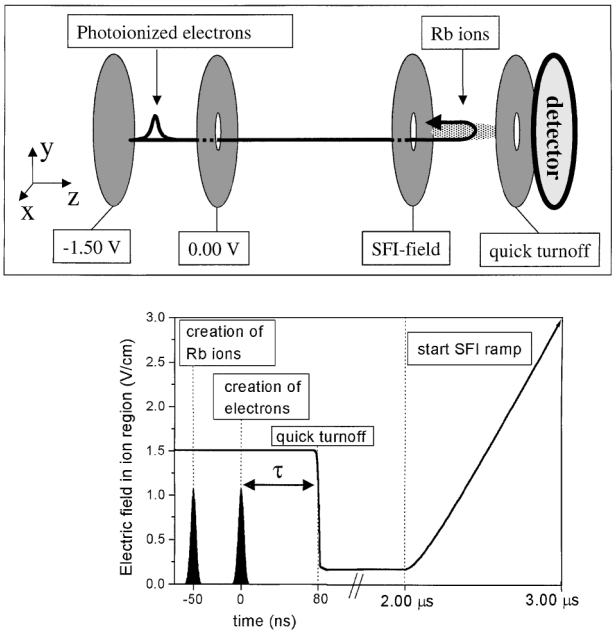

FIG. 2. Upper panel: experimental setup. A static electric field of 1.50 V/cm pushes electrons towards the rubidium ion region, where the ions await the electrons in an opposite electric field. The cathode plate is connected to a fast pulse generator so the field can be turned of within 0.4 to 9 ns. The anode plate is connected to a slow pulse generator for SFI detection. Lower panel: timing scheme of the experiment. The graph shows the electric field as a function of time in the ion region and when the electrons and ions were created by photoionization.

Most recombination processes are characterized by cross sections. In the PFR scheme it is more appropriate to give the volume in which the electron has to be at the moment of the quick turnoff to recombine with the ion. We define the interaction volume $V_{\rm int}$ as the volume of space for which an electron with an initial velocity $(0,0,v_z)$ will recombine with the ion after the electric field is ramped down to 200 mV/cm; it is not necessary to use a distribution in velocity due to the very low effective temperature of the electron source. This interaction volume can be estimated with the following formula:

$$N(\tau) = \rho_{\rm ion}\rho_e V_{\rm over} V_{\rm int}\,, \qquad (1)$$

where $N(\tau)$ is the number of recombinations at a certain delay (τ) of the quick turnoff, $\rho_{\rm ion}$ is the ion density, ρ_e is the electron density, $V_{\rm over}$ is the macroscopic overlap volume of the electron- and ion cloud, and $V_{\rm int} = \int_{-\infty}^{\infty} f(t'-\tau)v_{\rm int}(t')\,dt'$, where $f(t) = \sqrt{\frac{4\ln 2}{\pi\alpha^2}}\exp(\frac{-t^2 4\ln 2}{\alpha^2})$ is a function which describes

the time profile of the electron pulses (α is the duration of the electron pulses: 9 ns). Typically to have 15 recombination events per 5×10^4 electrons in an overlap volume of 0.02 mm^3 and an ion density of 2.5×10^6 cm^{-3} (these numbers were experimentally realized) this observed interaction volume is $(1.2 \pm 1.0) \times 10^{-10}$ cm^3. A theoretical estimate of V_{int} is obtained by classically solving Newton's equations, with a force equal to $\mathbf{F}(t) = q[\mathbf{E}(t) + \mathbf{v}(t) \times \mathbf{B}/c]$. The electric field ($\mathbf{E}$) is the superposition of the Coulomb potential of the ions and external field, $\mathbf{v}$ is the velocity of the electrons, and $\mathbf{B}$ is the magnetic field. An interaction volume of 0.25×10^{-10} cm^3 is found for a 9 ns electron pulse, which agrees very well with the estimated value from the experimental data. We note that the spatial extent of such an interaction volume corresponds to Rydberg states around $n \approx 200$. Note that the radius of the interaction volume is 2 orders of magnitude smaller than the average distance between neighboring ions, which means perturbations from unrecombined Rb^+ ions are not important for this experiment.

A detailed picture of the state distribution of the pulsed field recombined Rydberg atoms was obtained by selective field ionization (SFI) [6]. This technique makes use of the fact that Rydberg states of an atom can be ionized if a strong enough electric field is applied. The relation between the value of the electric field at which field ionization classically occurs and the principal quantum number n of a state is (in atomic units) $F = (\frac{E}{2})^2 = \frac{1}{16n^4}$. If the electric field is ramped in time and the field at which Rydberg atoms decay is monitored, the populated Rydberg states can be approximately deduced. To calculate the SFI spectrum, we propagated Newton's equation with the experimental ramp rate. In our experiment we use a field ramp of 2.00 V/cm in 1.80 μs, 2 μs after the fast field turnoff (Fig. 2). The field ramp pushes the field ionized electrons towards the cathode plate through which a hole was drilled and covered with a grid. The electrons are recorded by a set of microsphere plates (MSP's). In this way we record at which times, and hence at what field strengths, electrons are being field ionized. During the 2 μs after the quick turnoff and before the SFI ramp, effects of TBR and RR are ruled out since the rates of these processes are far too low at our densities (rate ~ 1 s^{-1}). Moreover, we checked for different delays of the SFI field what the total amount of recombinations was and this value did not have the tendency to increase for longer delays.

In the upper panel of Fig. 3 the SFI state distribution of the 0.4 ns turnoff is compared with theory. Note the excellent agreement between experiment and theory. Only at higher SFI fields (lower n) there is a small discrepancy between experiment and theory. This could be due to a slight difference in shape of the quick turnoff used in the calculation and in experiment. The shape of these traces shows that recombination to very highly excited states is most efficient. From the calculations an average principal

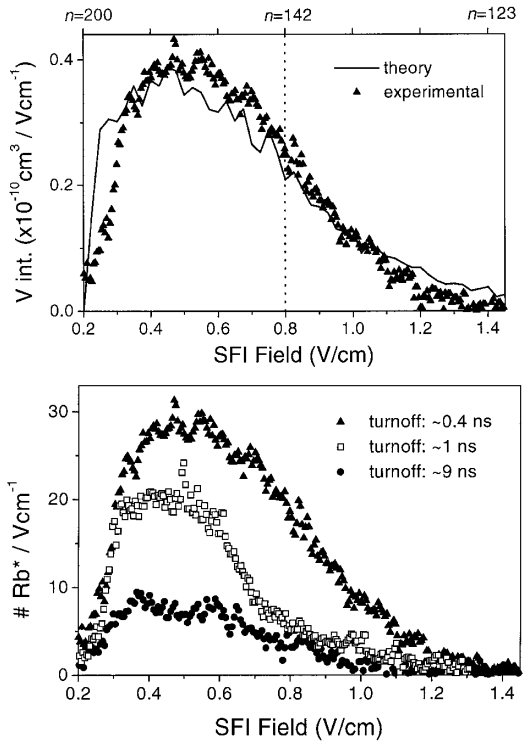

FIG. 3. Upper panel: calculated state distribution of the recombined Rydberg atoms compared with experimental state distribution. The experimentally determined interaction volume $[(1.0 \pm 0.7) \times 10^{-10}$ $cm^3]$ is varied within its error to optimize the comparison with theory ($V_{\text{int}} = 0.3 \times 10^{-10}$ cm^3). Lower panel: Recorded state distribution by the state selective field ionization (SFI) detection scheme. The three curves show the state distribution for different turnoff times.

quantum number can be retrieved: $\langle n \rangle = 170$, with $\Delta n = \sqrt{\langle n^2 \rangle - \langle n \rangle^2} = 23$. This agrees with the estimated interaction volume, which predicted recombined states on the order of $n = 200$. Calculations with and without core scattering showed no qualitative and quantitative difference in the recombined state distribution indicating that the nonhydrogenic Rb^+ core plays no role in the capture step.

The PFR dynamics was probed even further, by measuring the Rydberg state distribution for different turnoff times of the electric field from -1.50 to -0.20 V/cm at zero delay (Fig. 1d). In the lower panel of Fig. 3 three state distributions are depicted for different electric field turnoff times (averaged over 1000 laser shots). At the fastest field ramp used, not only more electrons are recombined, but also the captured state distribution extends to more deeply bound states. This can be explained by the fact that PFR relies on turning off the field before the electron can return to the saddle point. The change in energy of the electron from the ramp down of the field is $\Delta E = -e \int_{-\infty}^{\infty} (\frac{dF}{dt}) z(t)\, dt$ where $z(t)$ is the time dependent z coordinate of the electron. The time derivative of the field is a purely negative function. If $\frac{dF}{dt}$ is sharp, then there will be some trajectories for which $z(t)$ is purely negative over the

whole width of $\frac{dF}{dt}$. If $\frac{dF}{dt}$ is broad, $z(t)$ will go from positive, to negative, and back to positive over the width of $\frac{dF}{dt}$. Thus, the fast ramp downs (sharp $\frac{dF}{dt}$) give larger energy losses than the slow ramp downs (broad $\frac{dF}{dt}$). Moreover, the electron pulses in the PFR experiment are $\sim$9 ns long. Faster turnoffs use a smaller fraction of the electron pulses for recombination, resulting in a mismatch of the electron pulse duration and the duration of the fast field turnoff. We anticipate that making the electron pulses as short as the turnoff in time will increase the efficiency even more.

The connection of PFR can be made towards SRR in the low frequency domain. One moves from a limit where the optical period is much shorter than the time dynamics involved in the atomic system (e.g., the orbiting period of the captured electron), to a region where the field pulses have a duration of the order the time dynamics involved in the atomic system. Therefore this novel mechanism can be best described as an intermediate between TBR and SRR, in which no plasmas are required.

A potential application of this new recombination technique is the creation of atomic antihydrogen [10,11]. Observations of atomic antihydrogen are reported in Refs. [12,13], where a low number of antihydrogen atoms were observed with relativistic energies. So far the most promising schemes to produce cold atomic antihydrogen are based on a combined trap [14], where one relies on the interaction between positrons and antiprotons at very low relative velocities and low temperature. To date, the study of these recombination schemes is done with normal matter. In Ref. [10] such a combined trap is described, where typically $>10^5$ protons and 10^6 electrons (corresponding density: 10^8 cm^{-3}) in the combined trap were detected. However, up to now no successful experiments on the formation of neutral- or antimatter have been reported in this configuration. We foresee that the implementation of the third route of recombination, as introduced here, can in fact produce a sizable number of recombined neutral antimatter atoms (in a high Rydberg state) in the already realized combined trap. If the overlap volume is maximal (the antiproton plasma takes up the same volume as the positron plasma), the positron density is 10^{7-8} cm^{-3}, and the number of trapped antiprotons is 10^5, our scheme can produce 10^2–10^3 recombined antihydrogen atoms in a single experiment (assuming the same V_{int} as is observed in our measurements). The exact implementation of PFR for the experimental realization of atomic antihydrogen production is currently investigated, and beyond the scope of this Letter.

In summary, we have observed recombination of rubidium ions with free electrons with the use of fast electric field pulses. The process can be seen as the inverse process of field ionization. Efficiencies as high as 3×10^{-3} have been achieved and a simple improvement (due to the electron pulse duration mismatch) can raise the efficiency significantly. The observed effect can be understood with arguments which do not require mechanisms relying on the magnitude of the quantum defects of nonhydrogenic atoms, indicating that the PFR mechanism works for any atom. Moreover, we propose that our scheme is a promising avenue for the formation of neutral antimatter. Although we restricted the discussion in this Letter to the recombination of rubidium ions and electrons, the technique of PFR is in principle also applicable for the formation of neutral molecules, anions [15], and ion-pair states [16].

We are grateful to T. W. Hijmans for fruitful discussions on this experiment. C. W. and L. D. N. are supported by the Stichting Fundamenteel Onderzoek van de Materie (FOM) and the Nederlandse Organisatie voor Wetenschappelijk Onderzoek (NWO). F. R. is supported by the NSF.

[1] A. Muller, Commments At. Mol. Phys. **3**, 143 (1996).
[2] D. R. Bates, Phys. Rev. **77**, 718 (1950).
[3] G. Gabrielse, S. Rolston, L. Haarsma, and W. Kells, Phys. Lett. A **129**, 38 (1988).
[4] R. Flannery, *Atomic, Molecular, and Optical Physics Handbook* (AIP Press, Woodbury, New York, 1996).
[5] F. B. Yousif *et al.*, Phys. Rev. Lett. **67**, 26 (1991); U. Schramm *et al.*, Phys. Rev. Lett. **67**, 22 (1991); M. L. Rogelstad, F. B. Yousif, T. J. Morgan, and J. B. A. Mitchell, J. Phys. B **30**, 3913 (1997).
[6] T. F. Gallagher, *Rydberg Atoms* (Cambridge University Press, Cambridge, United Kingdom, 1994).
[7] T. F. Gallagher *et al.*, Phys. Rev. A **16**, 1098 (1977).
[8] E. W. Schlag, *ZEKE Spectroscopy* (Cambridge University Press, Cambridge, United Kingdom, 1998).
[9] D. Klar, M-W Ruf, and H. Hotop, Meas. Sci. Technol. **5**, 1248 (1994).
[10] G. Gabrielse *et al.*, Phys. Lett. B **455**, 311 (1999).
[11] G. Gabrielse, S. L. Rolston, and L. Haarsma, Phys. Lett. A **129**, 38 (1988); in *Non-Neutral Plasma Physics III*, edited by J. J. Bollinger, R. L. Spencer, and R. C. Davidson, AIP Conf. Proc. No. 498 (AIP, New York, 1999).
[12] G. Baur *et al.*, Phys. Lett. B **368**, 251 (1996).
[13] G. Blanford *et al.*, Phys. Rev. Lett. **80**, 3037 (1998).
[14] J. Walz *et al.*, Phys. Rev. Lett. **75**, 3257 (1995).
[15] C. Desfrancois, H. Abdoul-Carime, and J-P Schermann, Int. J. Mod. Phys. B **10**, 1339 (1996).
[16] J. D. D. Martin and J. W. Hepburn, Phys. Rev. Lett. **79**, 3154 (1997).